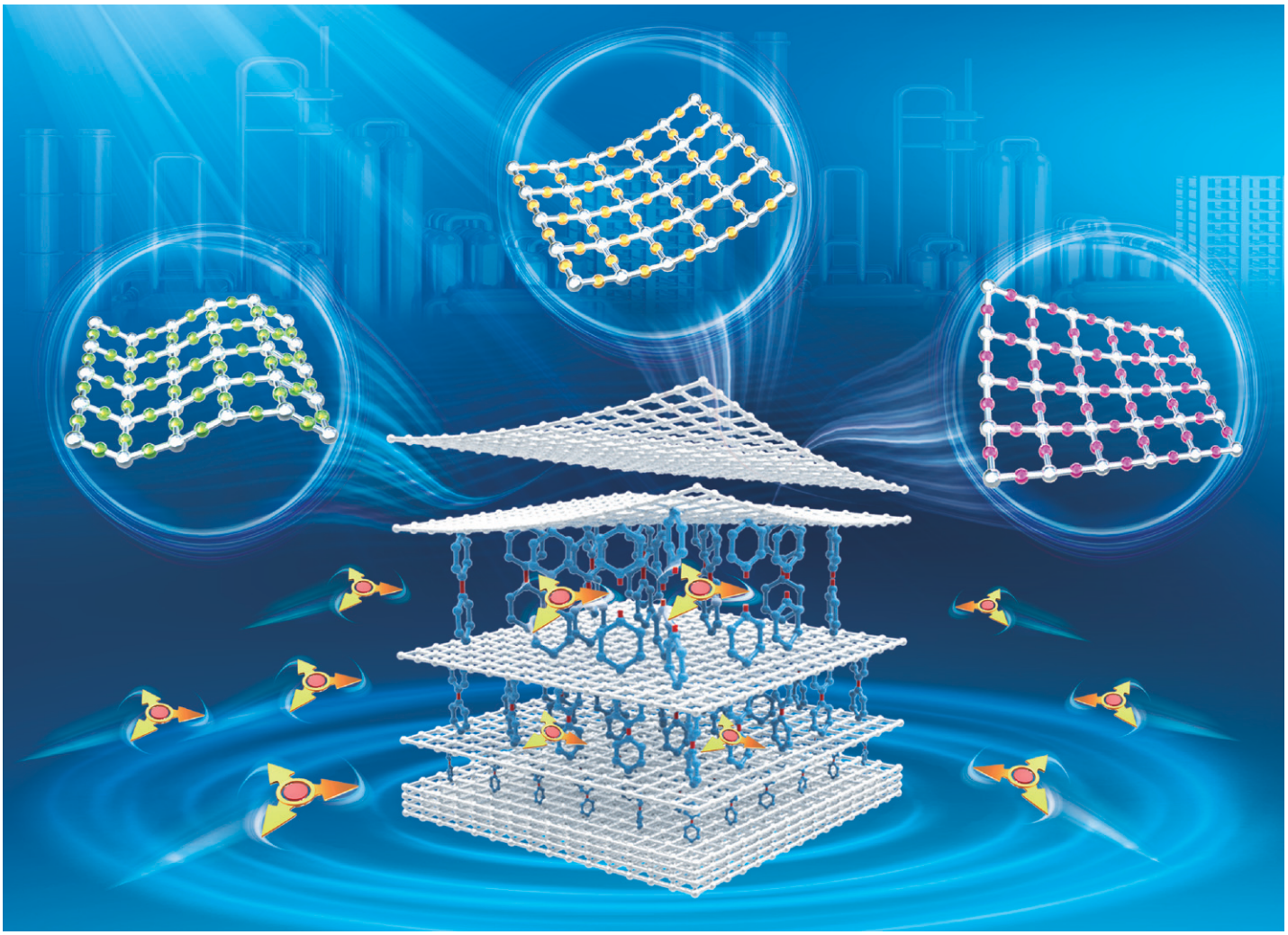

Showcasing research from Zhenxing Liang's laboratory, Key Laboratory on Fuel Cell Technology of Guangdong Province, School of Chemistry and Chemical Engineering, South China University of Technology, Guangzhou, China.

Ozonolysis–oxidation-driven top-down strategy for the target preparation of ultrathin 2D metal–organic framework monolayers

A novel chemical exfoliation method is developed for the target preparation of 2D MOF monolayers from the 3D pillar-layered MOFs.

As featured in:

See Zhipeng Xiang, Zhenxing Liang, Zhiyong Fu *et al.*, *Ind. Chem. Mater.*, 2024, **2**, 110.

ROYAL SOCIETY OF CHEMISTRY

Industrial Chemistry & Materials

Industrial Chemistry & Materials

ROYAL SOCIETY OF CHEMISTRY

PAPER

View Article Online
View Journal | View Issue

Cite this: *Ind. Chem. Mater.*, 2024, **2**, 110

Ozonolysis–oxidation-driven top-down strategy for the target preparation of ultrathin 2D metal–organic framework monolayers†

Baoliu Zhuo,‡[a] Aidong Tan,‡[ab] Zhipeng Xiang,*[a] Jinhua Piao,[c] Wenhao Zheng,[a] Kai Wan,[a] Zhenxing Liang*[a] and Zhiyong Fu*[a]

Two-dimensional metal–organic-framework (2D MOF) nanosheets with a modular nature and tunable structures exhibit a bright future for sensors, separation, and catalysis. Developing ultrathin 2D MOF nanosheets with unique physical and chemical properties is urgently required but very challenging. Although the chemical exfoliation strategy has been regarded as a promising way to exfoliate large amounts of three-dimensional (3D) pillar-layered MOFs, this method still faces many problems and remains insufficient. In this study, a novel chemical exfoliation method is developed for the target preparation of 2D MOF monolayers from the 3D pillar-layered MOFs. The Co/Zn/Cu-MOFs with a pillar ligand of *trans*-1,2-bis(4-pyridyl)ethylene (bipyen) are subjected to be broken by the cleavage of C=C bonds in the bipyen ligands *via* an ozone oxidation reaction. As chemical exfoliation is processed *via* the oxidation of the pillar ligand by ozone, the thickness of the 2D MOFs can be tuned by the control of oxidation time and the obtained 2D Co/Zn/Cu-MOF monolayers are functionalized with a –COOH group. This study provides an effective and general chemical exfoliation method to prepare monolayer MOFs from the 3D pillar-layered MOFs with bipyen as the pillar ligand.

Keywords: 3D pillar-layered MOFs; Ultrathin 2D MOF monolayers; Top-down strategy; Chemical exfoliation; Ozonolysis–oxidation.

Received 13th April 2023,
Accepted 7th June 2023

DOI: 10.1039/d3im00045a

rsc.li/icm

1 Introduction

Two-dimensional (2D) materials with atomic or molecular thickness levels have attracted considerable attention owing to their unique physical and chemical properties in many areas, such as electronics, sensors, biomedicine, catalysis, separation, energy conversion, and storage.[1–7] As an emerging important family of multifunctional 2D materials, 2D metal–organic-framework (2D MOF) nanosheets with a modular nature and tunable structures, including structural diversity, large specific surface area, high porosity, and controllable pore size, have a bright future for many applications, such as sensors, separation, and catalysis.[8–13] These attractive features and promising applications have endowed 2D MOF nanosheets as a new competitive member of 2D nanomaterials. Therefore, the precise synthesis of ultrathin 2D MOF nanosheets with controllable multiple aspect ratios and integrated phase structure has received intensive interest in the past years.[11,14–17]

In general, two strategies have been developed for the synthesis of 2D MOF nanosheets.[18–20] One is the bottom-up approach, by which the MOF nanosheets are directly and controllably assembled by the corresponding metal ions and organic linkers in solution.[21–23] However, the bottom-up approach is largely limited by the reaction conditions, which cannot be applied as a universal method. The other one is the top-down approach, by which 2D MOF nanosheets are obtained *via* physical or chemical exfoliation of the bulk MOF.[24–26] Compared with the bottom-up synthesis strategy, the top-down method is more widely applicable. For example, the way of physical exfoliation has been regarded as the most powerful and scalable approach for the exfoliation of almost all 2D layered MOFs through exogenous physical force or solvent mediation to regulate the interlayer interaction.[27–30] While the chemical exfoliation strategy has been regarded as

[a] *Key Laboratory on Fuel Cell Technology of Guangdong Province, School of Chemistry and Chemical Engineering, South China University of Technology, Guangzhou 510641, P.R. China. E-mail: xzp20209094@scut.edu.cn, zliang@scut.edu.cn, zyfu@scut.edu.cn*
[b] *Institute of Energy Power Innovation, North China Electric Power University, Beijing, 102206, P.R. China*
[c] *School of Food Science and Engineering, South China University of Technology, Guangzhou 510641, P.R. China*

† Electronic supplementary information (ESI) available. See DOI: https://doi.org/10.1039/d3im00045a

‡ These authors contributed equally to this work.

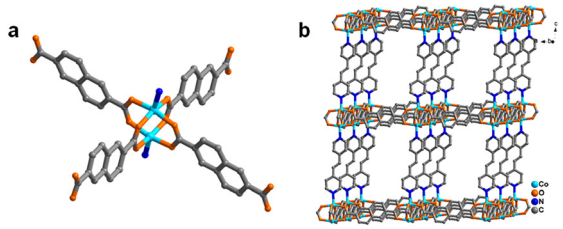

Fig. 1 (a) Coordinated structure of the Co-MOF with H_2NDC as layer ligands; (b) three-dimensional pillared structure of the Co-MOF with bipyen as pillar ligands.

a promising way to the exfoliation of 3D pillar-layered MOFs *via* cleaving the covalent bonds of their pillar ligands by chemical reactions.[27,31,32] For example, ultrathin 2D MOF nanosheets are reported to be effectively prepared by an electrochemical–chemical exfoliation approach.[33] The electrochemically generated oxygen can *in situ* oxidize and remove the pillar ligand of 2,3-dihydroxy-1,4-benzenedicarboxylic in a 3D pillar-layered MOF. An intercalation-chemical exfoliation method has been developed to build 2D MOF nanosheets.[34] 4,4-Dipyridyl disulfide was first intercalated into the layered porphyrinic MOF networks by coordination bonding with the metal sites, resulting in a 3D pillar-layered structure. Then, 2D MOF nanosheets can be obtained *via* selectively cleaving the disulfide bond. While the way of chemical exfoliation 3D pillar-layered MOFs makes much progress, it still faces various problems, such as the complex selective breakage, structural modification of the pillar ligands between the layers, and maintaining the stability of the coordinate bonds within a layer.[32] Considering the large amounts of 3D pillar-layered MOFs being as potential precursors, it is highly desirable and challenging to develop a facile and universal chemical exfoliation method for the target dissociation of 3D pillar-layered MOFs.

Herein, a new chemical exfoliation method is developed with ozone as oxidant for the exfoliation of 3D pillar-layered MOF. A Co-MOF is selected as model precursor with *trans*-1,2-bis(4-pyridyl)ethylene (bipyen) as the pillar ligands. Its 3D structure is subjected to be broken by the cleavage of C=C bonds in the bipyen ligands *via* an ozone oxidation reaction. Interestingly, this kind of chemical exfoliation can be tuned by the control of oxidation time. Monolayer 2D Co-MOF nanosheets with –COOH functionalization are successfully obtained after the chemical exfoliation of 90 min. In addition, this method is effective for similar 3D pillar-layered Zn/Cu-MOF precursors with bipyen as pillar ligands.

2 Results and discussion

For the fabrication of 2D Co-MOF nanosheets, a Co-MOF with the 3D pillar-layered structure is prepared as a precursor by a hydrothermal reaction of cobalt metal salt, pillar ligand, and layer ligand in deionized water at 180 °C for 48 h, according to the previous report.[35] In its structure, the 2D bilayer is constructed by the connections of the layer ligand 2,6-naphthalenedicarboxylic acid (H_2NDC) and Co(II) ions (Fig. 1a). Further layer-by-layer assembly linked by the pillar ligand *trans*-1,2-bis(4-pyridyl)ethylene (bipyen) results in the final 3D pillar-layered Co-MOF framework (Fig. 1b).

The chemical exfoliation process of the 3D pillar-layered Co-MOF is illustrated in Scheme 1 in which the C=C connection of the pillar ligand bipyen is broken by an ozone oxidation reaction.[36–38] Two isonicotinic acid units generate while ozone is bubbled into the dispersion solution of the 3D Co-MOF at 0 °C in DMF for different durations (Scheme 1, red square). The effective breakage of the C=C bonds among ozone oxidation reaction is confirmed by the ^{1}H nuclear magnetic resonance (NMR) spectroscopy. After the ozone treatment, the oxidation product exhibits the same peaks as those of theoretical ^{1}H NMR spectra of isonicotinic acid, indicating the successful breakage of C=C bonds of the pillar ligand bipyen (Fig. S1, ESI†). As a result, a 2D bilayer structural Co-MOF nanosheet is generated by the coordination of Co(II) ions to the isonicotinic acid ligands locating on both sides (Scheme 1).

To investigate the chemical exfoliation process, scanning electron microscopy (SEM) images, powder X-ray diffraction (PXRD), transition electron microscopy (TEM), and atomic force microscope (AFM) were employed to characterize the morphology evolution of the Co-MOFs under different reaction durations. Scanning electron microscopy (SEM)

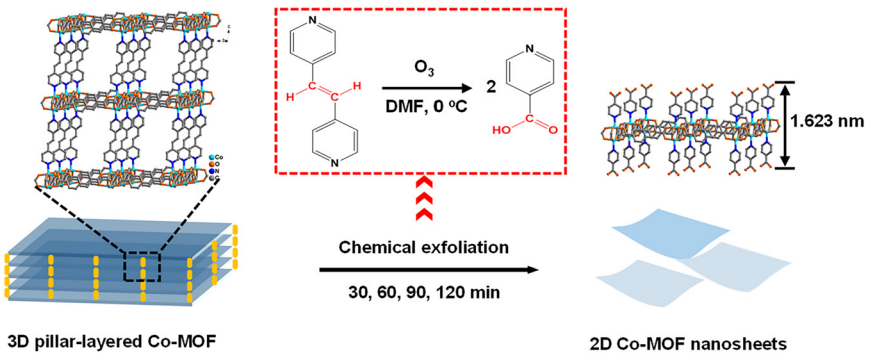

Scheme 1 Schematic illustration of the chemical exfoliation of the 3D pillar-layered Co-MOF precursor.

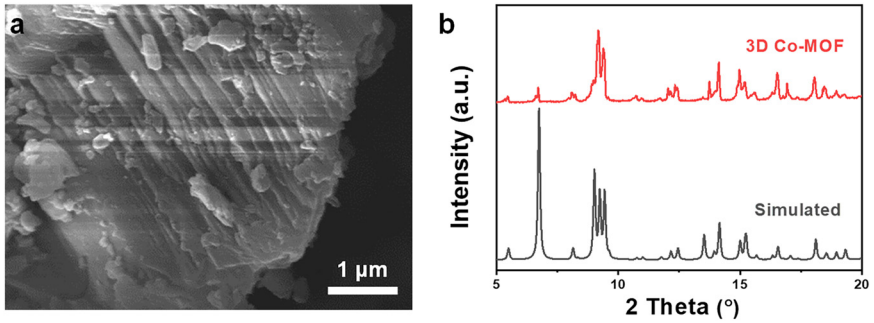

Fig. 2 (a) SEM image and (b) experimental and simulated XRD patterns of the 3D pillar-layered Co-MOF.

images reveal that the 3D pillar-layered Co-MOF has a block shape morphology with conspicuous multilayer structure (Fig. 2a and S2, ESI†). PXRD data confirms phase purity of the prepared 3D Co-MOF precursor, which exhibit the same diffraction peaks as those of simulated pattern (Fig. 2b). The diffraction peak located at 2θ = 5.5° can be attributed to the (001) crystal plane of the 3D Co-MOFs, corresponding to the crystal face composed of the pillar ligand bipyen.

TEM images indicate that the Co-MOF precursor still maintains its 3D pillar-layered structure after ozone treatment for 30 min (Fig. 3a). As the reaction duration increases to 60 min, 2D Co-MOF nanosheets are observed (Fig. 3b). Moreover, thinner 2D Co-MOF nanosheets are obtained while the time prolongs from 60 min to 90 min (Fig. 3c), displaying the successful exfoliation of 3D pillar-layered Co-MOF. It is observed that the obtained nanosheets exhibit wrinkled and curved morphologies, showing the characteristics of ultrathin thickness. In addition, some small sized nanosheets are adsorbed on the 2D Co-MOF nanosheet due to the electrostatic adsorption. Finally, the 2D Co-MOF nanosheets exhibit low lateral dimension and even aggregated together to form nanoparticles while the duration time prolongs to 120 min (Fig. 3d). This may be attributed to the destruction of the layered structure by the excessive ozone. These identifications are further approved by the XRD patterns of exfoliated Co-MOFs under different reaction duration. It is observed that the intensity of the diffraction peak at 5.5° gradually decreased and finally disappeared as the ozone treatment time going by (Fig. 3e). This indicates the loss of (001) crystal plane while the C=C bonds in pillar ligand bipyen are broken. As shown in the atomic force microscope (AFM) data, the thickness of the 2D Co-MOF nanosheet (1.6 nm, Fig. 3g) is close to the simulation value of the theoretical single-layer crystal (Scheme 1). These results show that the chemical exfoliation process of this 3D pillar-layered MOF can be fine-tuned by the control of ozone treatment duration.

For the chemical exfoliation mechanism, the formed 2D Co-MOF nanosheets are expected to functionalize with –COOH groups on their surface. As shown in Fig. 4a, the 2D Co-MOF nanosheet exhibits a negative zeta potential of −25 mV than that of its 3D Co-MOF precursor (−4.5 mV), indicating more negative charge feature due to the dissociation of the –COOH groups. To verify the presence of –COOH groups, the 3D Co-MOF and 2D Co-MOF nanosheets are dissolved in DCl, and solvents containing the organic

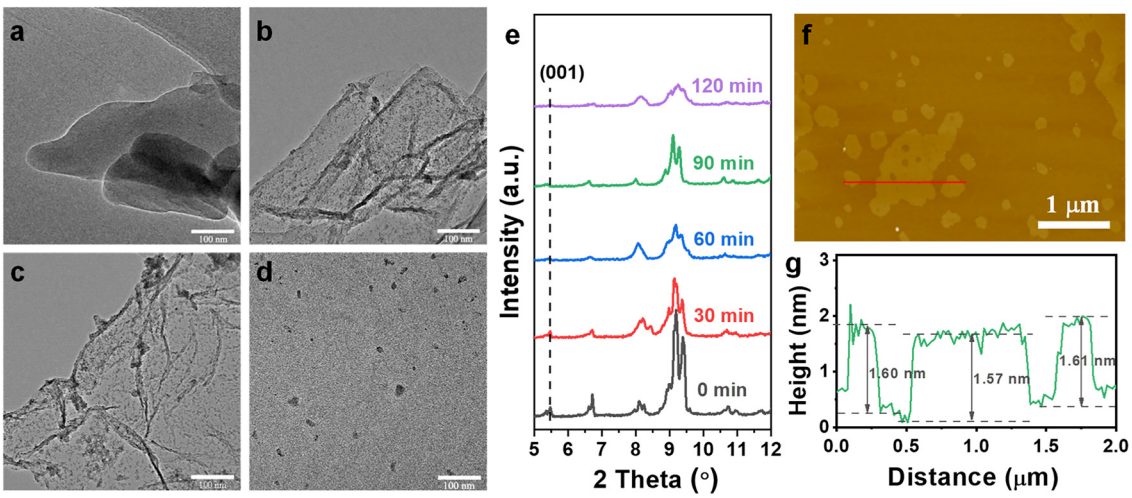

Fig. 3 TEM images of the 3D Co-MOF subjected to a chemical exfoliation for different reaction durations of (a) 30 min, (b) 60 min, (c) 90 min, and (d) 120 min; (e) XRD patterns of the 3D Co-MOF subjected to a chemical exfoliation for different reaction durations; (f) AFM image of the 3D Co-MOF being exfoliated for 90 min; and (g) the corresponding thickness of the resulted nanosheets.

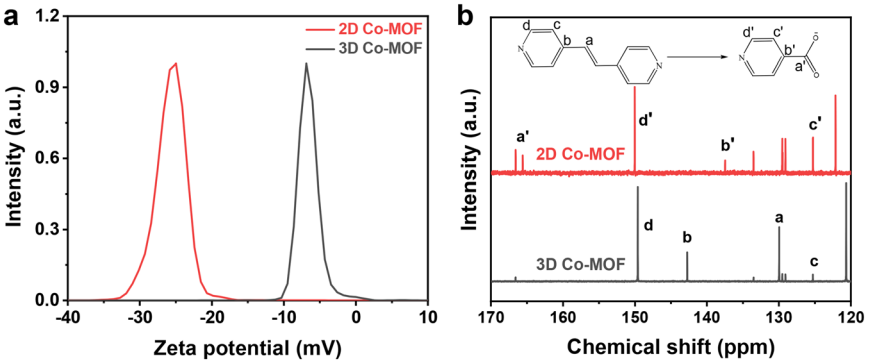

Fig. 4 (a) Zeta potential of the 3D Co-MOF precursor and 2D Co-MOF nanosheets; (b) the ^{13}C NMR spectra of the solvents derived from 3D Co-MOF precursor and 2D Co-MOF nanosheet.

ligands are measured by the ^{13}C NMR spectroscopy. It is seen from Fig. 4b that the chemical shifts at 125.3, 129.9, 142.7, and 149.6 ppm correspond to the pillar ligand of bipyen, while the chemical shifts at 125.4, 137.5, 150.0, and 165.6 ppm correspond to the isonicotinic acid. These results suggest the functionalization of the –COOH groups on the 2D Co-MOF nanosheet.

To test the generality of this method, two similar 3D pillar-layered MOFs (Zn-MOF and Cu-MOF, as shown in Fig. S3, ESI†) with bipyen as a pillar ligand were prepared for the chemical exfoliation. The corresponding XRD patterns of the 3D Zn-MOF and 3D Cu-MOF further confirm the crystal structures (Fig. S4, ESI†). It can be seen from Fig. 5a and b that the 3D Zn-MOF and 3D Cu-MOF possess block shape morphology with a conspicuous multilayer structure. 2D nanosheet morphology is observed in Fig. 5c and d after the chemical exfoliation for 90 min, confirming the successful chemical exfoliation. The EDS mapping results show that the 2D Zn-MOF and 2D Cu-MOF are composed of C, H, O, and Zn or Cu (Fig. S5†), and the 2D nanosheet structures were confirmed by comparing with the simulated XRD patterns of the 2D Zn-MOF and 2D Cu-MOF (Fig. S6, ESI†). It was found that the 2D Zn-MOF has a thickness of 1.6 nm and the 2D Cu-MOF has a thickness of around 2.0 nm (Fig. 6), displaying their monolayer feature. Moreover, the obtained 2D Zn-MOF and 2D Cu-MOF nanosheets also exhibit negative zeta potentials than that of the 3D Zn-MOF and 3D Cu-MOF (Fig. S7, ESI†), indicating the functionalization of –COOH groups.

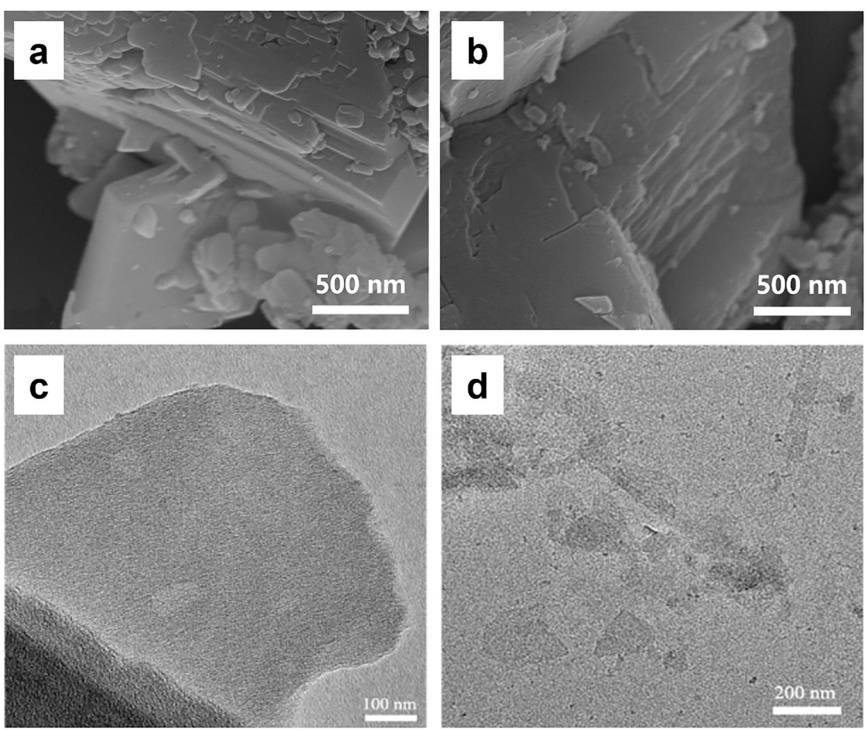

Fig. 5 SEM images of the 3D pillar-layered (a) Zn-MOF precursor and (b) Cu-MOF precursor and TEM images of the (c) 2D Zn-MOF nanosheet and (d) 2D Cu-MOF nanosheet.

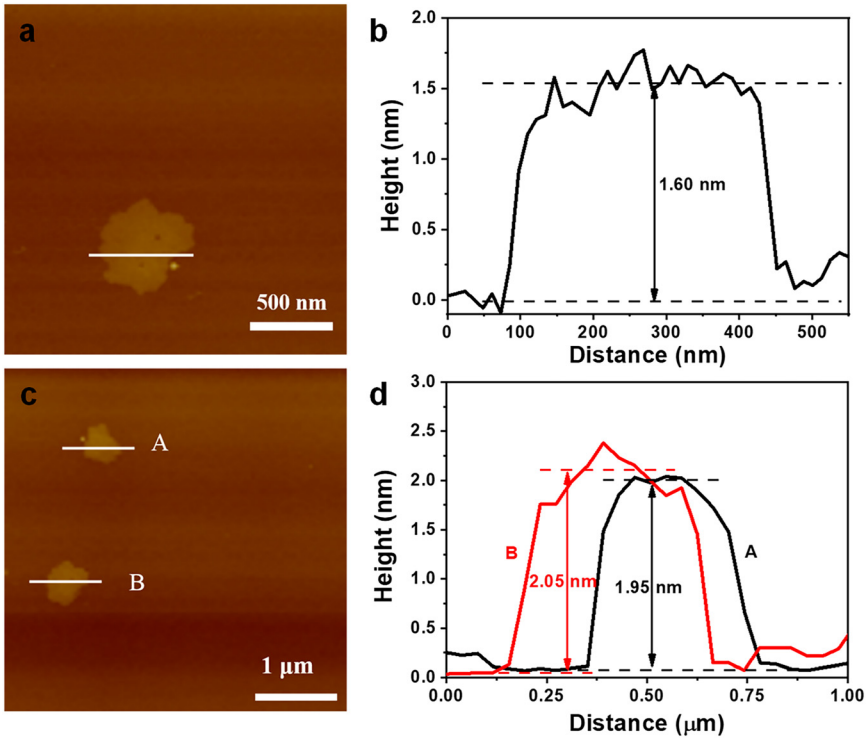

Fig. 6 AFM images and the corresponding thickness of the (a) and (b) 2D Zn-MOF nanosheet and (c) and (d) 2D Cu-MOF nanosheet.

3 Conclusions

In summary, the monolayer 2D Co/Zn/Cu-MOFs nanosheets functionalized with –COOH groups were exfoliated from 3D pillar-layered MOFs by the convenient chemical exfoliation method. The 3D pillar-layered MOFs were easy to flake off *via* cleaving the covalent bonds of the pillar ligands by ozonolysis oxidation. Its chemical process can be controlled by the oxidation duration of the pillar ligand with ozone. This study provides an effective and generality chemical exfoliation method to prepare monolayer MOFs from the 3D pillar-layered MOFs with bipyen as a pillar ligand.

4 Experimental section

4.1 Chemicals

$Co(NO_3)_2{\cdot}6H_2O$ (AR, >99.0%, Aladdin), $Zn(NO_3)_2{\cdot}2H_2O$ (AR, >99.0%, Guangdong Guanghua Chemical Factory Co., Ltd.), $Cu(NO_3)_2{\cdot}2.5H_2O$ (AR, >99.0%, Guangdong Guanghua Chemical Factory Co., Ltd.), *trans*-1,2-bis(4-pyridyl)ethylene (Bipyen, 98%, Aladdin), *trans*-1,4-cyclohexanedicarboxylic acid (H_2CDC, 97%, Aladdin), 2,6-naphthalenedicarboxylic acid (H_2NDC, 98%, Energy Chemical), acetone (AR, >99.0%, Guangdong Guanghua Chemical Factory Co., Ltd.), *N*,*N*-dimethylformamide (DMF, AR, >99.5%, Guangdong Guanghua Sci-Tech Co., Ltd.), ethanol (AR, >99.5%, Guangdong Guanghua Sci-Tech Co., Ltd.), hexane (AR, >99.5%, Guangdong Guanghua Sci-Tech Co., Ltd.), and potassium iodide (AR, >99.0%, Aladdin). All the chemicals were obtained from commercial sources and used as received.

4.2 Materials preparation

Preparation of 3D pillar-layered MOFs of $[Co_3(NDC)_3(bipyen)_{1.5}]{\cdot}H_2O$ (3D Co-MOF). The synthesis of the 3D Co-MOF was carried out according to the previous report.[35] Typically, 87.3 mg $Co(NO_3)_2{\cdot}6H_2O$ (0.3 mmol), 64.9 mg H_2NDC (0.3 mmol), 54.7 mg bipyen (0.3 mmol) were dissolved in 15 mL H_2O and reacted in a 25 mL Teflon reactor at 180 °C for 48 h. The dark green product was collected by filtration and washed with H_2O, ethanol, and acetone, then vacuum-dried at 70 °C overnight. The productivity was only 5%.

Preparation of 3D pillar-layered MOFs of $Zn(NDC)(bipyen)_{0.5}{\cdot}2.5DMF{\cdot}0.5H_2O$ (3D Zn-MOF). The synthesis of the 3D Zn-MOF was carried out according to the previous report.[39] Generally, 331.4 mg $Zn(NO_3)_2{\cdot}2H_2O$ (1.47 mmol), 317.8 mg H_2NDC (1.47 mmol), and 134.8 mg bipyen (0.74 mmol) were dissolved in 60 mL DMF and reacted in a 150 mL distillation bottle at 100 °C for 24 h. The colorless product was collected by filtration and washed with DMF and hexane, then vacuum-dried at 70 °C overnight. The productivity is 75%.

Preparation of 3D pillar-layered MOFs of $Cu_4(CDC)_4(bipyen)$ (3D Cu-MOF). The synthesis of the 3D Cu-MOF was carried out according to the previous report.[40] Generally, 56.3 mg $Cu(NO_3)_2{\cdot}2.5H_2O$ (0.242 mmol), 63.0 mg H_2CDC (0.366 mmol), and 22.1 mg bipyen (0.121 mmol) were

dissolved in 15 mL H_2O and reacted in a 25 mL Teflon reactor at 80 °C for 72 h. The blue-green product was collected by filtration and washed with H_2O, ethanol, and acetone, then vacuum-dried at 70 °C overnight. The productivity is only 10%.

Preparation of 2D MOF nanosheets. The 3D pillar-layered MOFs were first ball milling to obtain a uniform size thus facilitate subsequent chemical exfoliation process. The 3D pillar-layered MOFs were still remaining the pillar-layered structure after ball milling step. The ball milling process was as follows: 50 mg 3D MOFs and 15.0 mL ethanol were added into the agate jar and ball milling at 400 rpm min^{-1} for 2 h. Then, the obtained dispersion was filtered and vacuum-dried at 70 °C overnight. In a typical ozone oxidation experiment, 15 mg of the above ball-milled 3D MOF was dispersed in 20 mL DMF under sonication in a 50 mL two-necked round bottom flask and then cooled to 0 °C. Then, the ozone gas flux (5.28 mmol h^{-1}) was passed into the mixture for 60 min, 90 min, and 120 min under sonication (100 W, 60 kHz), and the exhaust gas was absorbed by potassium iodide solution. The exfoliated ultrathin 2D MOF nanosheets were collected from the upper colloidal suspension after sedimentation for 2 h by centrifugal separation (12 000 rpm min^{-1} for 15 min) and then dispersed in ethanol for freeze-drying.

4.3 Physicochemical characterization

PXRD were carried out on an X-ray diffractometer (Cu Kα radiation, 40 kV, 40 mA, D8 Advance, Bruker, Germany) at a scan rate of 0.02° per second in the 2θ range from 5° to 30°. The morphology and microstructures were characterized by scanning electron microscopy (SEM, SU8220, Japan) under an acceleration voltage of 10.0 kV and transmission electron microscopy (TEM, JEM-2100HR, JEOL, Japan) at an accelerating voltage of 200 kV. Atomic force microscopy (AFM) images were obtained by a Bruker Multimode 8 device. NMR spectra were recorded on Bruker-500 (500 MHz for ^1H, 500 MHz for ^{13}C) instruments internally referenced to the $SiMe_4$ signal. Zeta potential was performed by zeta-potential tester (90 Plus, Brookhaven Instruments Corporation, America).

4.4 Ozone treatment of *trans*-1,2-bis(4-pyridyl)ethylene

First, 10 mg *trans*-1,2-bis(4-pyridyl)ethylene was dissolved in 20 mL DMF in a 50 mL two-necked round bottom flask. Second, the ozone gas (5.28 mmol h^{-1}) was bubbled into the solution for 40 min under sonication in an ice-water bath. Then, the product was collected by evaporating the DMF and analyzed by ^1H NMR.

Conflicts of interest

The authors declare no conflict of interest.

Acknowledgements

The work described in this paper was jointly supported by the National Natural Science Foundation of China (No. U22A20417, 21903026, 21975081, 21975079, 22178126, 22108085), China Postdoctoral Science Foundation (2022M711196), Science and Technology Program of Guangzhou (2023A04J1357) and the SRP Program.

References

1 P. V. Shinde, A. Tripathi, R. Thapa and C. Sekhar Rout, Nanoribbons of 2D materials: A review on emerging trends, recent developments and future perspectives, *Coord. Chem. Rev.*, 2022, **453**, 214335.
2 X. Zhang, A. Chen, L. T. Chen and Z. Zhou, 2D materials bridging experiments and computations for electro/photocatalysis, *Adv. Energy Mater.*, 2022, **12**, 2003841.
3 S. J. Kang, D. H. Lee, J. Kim, A. Capasso, H. S. Kang, J. W. Park, C. H. Lee and G. H. Lee, 2D semiconducting materials for electronic and optoelectronic applications: Potential and challenge, *2D Mater.*, 2020, **7**, 022003.
4 J. X. Liu, Y. X. Chen, X. L. Feng and R. H. Dong, Conductive 2D conjugated metal–organic framework thin films: Synthesis and functions for (opto-)electronics, *Small Struct.*, 2022, **3**, 2100210.
5 J. Yan, T. Liu, X. Liu, Y. Yan and Y. Huang, Metal-organic framework-based materials for flexible supercapacitor application, *Coord. Chem. Rev.*, 2022, **452**, 214300.
6 R. J. Wei, P. Y. You, H. Duan, M. Xie, R. Q. Xia, X. Chen, X. Zhao, G.-H. Ning, A. I. Cooper and D. Li, Ultrathin metal–organic framework nanosheets exhibiting exceptional catalytic activity, *J. Am. Chem. Soc.*, 2022, **144**, 17487–17495.
7 S. Jindal and J. N. Moorthy, Zwitterionic luminescent 2D metal-organic framework nanosheets (LMONs): Selective turn-on fluorescence sensing of dihydrogen phosphate, *Inorg. Chem.*, 2022, **61**, 3942–3950.
8 L. T. Zhang, Y. Zhou and S. T. Han, The role of metal-organic frameworks in electronic sensors, *Angew. Chem., Int. Ed.*, 2021, **60**, 15192–15212.
9 X. Zhang, Y. Li, C. Van Goethem, K. Wan, W. Zhang, J. S. Luo, I. F. J. Vankelecom and J. Fransaer, Electrochemically assisted interfacial growth of MOF membranes, *Matter*, 2019, **1**, 1285–1292.
10 S. Xie, W. Monnens, K. Wan, W. Zhang, W. Guo, M. Xu, I. F. J. Vankelecom, X. Zhang and J. Fransaer, Cathodic electrodeposition of MOF films using hydrogen peroxide, *Angew. Chem., Int. Ed.*, 2021, **60**, 24950–24957.
11 G. Chakraborty, I. H. Park, R. Medishetty and J. J. Vittal, Two-dimensional metal-organic framework materials: Synthesis, structures, properties and applications, *Chem. Rev.*, 2021, **121**, 3751–3891.
12 H. Zhou, L. Zhang, G. Wang, Y. Zhang, X. Wang, M. Li, F. Fan, Y. Li, T. Wang, X. Zhang and Y. Fu, Fabrication of 2D metal-organic framework nanosheets with highly colloidal

stability and high yield through coordination modulation, *ACS Appl. Mater. Interfaces*, 2021, **13**, 39755–39762.

13 L. L. Dang, T. T. Zhang, T. Chen, Y. Zhao, X. Gao, F. Aznarez, L. F. Ma and G. X. Jin, Selective synthesis and structural transformation of a 4-ravel containing four crossings and featuring Cp*Rh/Ir fragments, *Angew. Chem., Int. Ed.*, 2023, **62**, 202301516.

14 W. Liu, R. Yin, X. Xu, L. Zhang, W. Shi and X. Cao, Structural engineering of low-dimensional metal-organic frameworks: Synthesis, properties, and applications, *Adv. Sci.*, 2019, **6**, 1802373.

15 X. Xiao, L. Zou, H. Pang and Q. Xu, Synthesis of micro/nanoscaled metal-organic frameworks and their direct electrochemical applications, *Chem. Soc. Rev.*, 2020, **49**, 301–331.

16 X. C. Cai, Z. X. Xie, D. D. Li, M. Kassymova, S. Q. Zang and H. L. Jiang, Nano-sized metal-organic frameworks: Synthesis and applications, *Coord. Chem. Rev.*, 2020, **417**, 213366.

17 G. Cai, P. Yan, L. Zhang, H. C. Zhou and H. L. Jiang, Metal-organic framework-based hierarchically porous materials: Synthesis and applications, *Chem. Rev.*, 2021, **121**, 12278–12326.

18 K. A. S. Usman, J. W. Maina, S. Seyedin, M. T. Conato, L. M. Payawan, L. F. Dumée and J. M. Razal, Downsizing metal-organic frameworks by bottom-up and top-down methods, *NPG Asia Mater.*, 2020, **12**, 58.

19 C. L. Ruiz-Zambrana, M. Malankowska and J. Coronas, Metal organic framework top-down and bottom-up patterning techniques, *Dalton Trans.*, 2020, **49**, 15139–15148.

20 Y. S. Zheng, F. Z. Sun, X. Han, J. L. Xu and X. H. Bu, Recent progress in 2D metal-organic frameworks for optical applications, *Adv. Opt. Mater.*, 2020, **8**, 2000110.

21 V. Rubio-Gimenez, M. Galbiati, J. Castells-Gil, N. Almora-Barrios, J. Navarro-Sanchez, G. Escorcia-Ariza, M. Mattera, T. Arnold, J. Rawle, S. Tatay, E. Coronado and C. Marti-Gastaldo, Bottom-up fabrication of semiconductive metal-organic framework ultrathin films, *Adv. Mater.*, 2018, **30**, 1704291.

22 Y. Wang, L. J. Li, L. T. Yan, X. Gu, P. C. Dai, D. D. Liu, J. G. Bell, G. M. Zhao, X. B. Zhao and K. M. Thomas, Bottom-up fabrication of ultrathin 2D Zr metal-organic framework nanosheets through a facile continuous microdroplet flow reaction, *Chem. Mater.*, 2018, **30**, 3048–3059.

23 Y. Lin, H. Wan, D. Wu, G. Chen, N. Zhang, X. Liu, J. Li, Y. Cao, G. Qiu and R. Ma, Metal-organic framework hexagonal nanoplates: Bottom-up synthesis, topotactic transformation, and efficient oxygen evolution reaction, *J. Am. Chem. Soc.*, 2020, **142**, 7317–7321.

24 M. P. Jian, R. S. Qiu, Y. Xia, J. Lu, Y. Chen, Q. F. Gu, R. P. Liu, C. Z. Hu, J. H. Qu, H. T. Wang and X. W. Zhang, Ultrathin water-stable metal-organic framework membranes for ion separation, *Sci. Adv.*, 2020, **6**, 3998.

25 Y. Zhou, P. Yan, S. Zhang, Y. Zhang, H. Chang, X. Zheng, J. Jiang and Q. Xu, CO_2 coordination-driven top-down synthesis of a 2D non-layered metal-organic framework, *Fundam. Res.*, 2021, **2**, 674–681.

26 C. Kutzscher, A. Gelbert, S. Ehrling, C. Schenk, I. Senkovska and S. Kaskel, Amine assisted top-down delamination of the two-dimensional metal-organic framework $Cu_2(bdc)_2$, *Dalton Trans.*, 2017, **46**, 16480–16484.

27 W. W. Zhao, J. L. Peng, W. K. Wang, S. J. Liu, Q. Zhao and W. Huang, Ultrathin two-dimensional metal-organic framework nanosheets for functional electronic devices, *Coord. Chem. Rev.*, 2018, **377**, 44–63.

28 J. G. Duan, Y. S. Li, Y. C. Pan, N. Behera and W. Q. Jin, Metal-organic framework nanosheets: An emerging family of multifunctional 2D materials, *Coord. Chem. Rev.*, 2019, **395**, 25–45.

29 T. Zheng, X. Kang and Z. Liu, Effective enhancement of capacitive performance by the facile exfoliation of bulk metal-organic frameworks into 2D-functionalized nanosheets, *Nanoscale*, 2021, **13**, 13273–13284.

30 Y. Peng, Y. Li, Y. Ban and W. Yang, Two-dimensional metal-organic framework nanosheets for membrane-based gas separation, *Angew. Chem., Int. Ed.*, 2017, **56**, 9757–9761.

31 L. Li, J. D. Yi, Z. B. Fang, X. S. Wang, N. Liu, Y. N. Chen, T. F. Liu and R. Cao, Creating giant secondary building layers *via* alkali-etching exfoliation for precise synthesis of metal-organic frameworks, *Chem. Mater.*, 2019, **31**, 7584–7589.

32 J. H. Deng, Y. Q. Wen, J. Willman, W. J. Liu, Y. N. Gong, D. C. Zhong, T. B. Lu and H. C. Zhou, Facile exfoliation of 3D pillared metal-organic frameworks (MOFs) to produce MOF nanosheets with functionalized surfaces, *Inorg. Chem.*, 2019, **58**, 11020–11027.

33 J. Huang, Y. Li, R. K. Huang, C. T. He, L. Gong, Q. Hu, L. Wang, Y. T. Xu, X. Y. Tian, S. Y. Liu, Z. M. Ye, F. Wang, D. D. Zhou, W. X. Zhang and J. P. Zhang, Electrochemical exfoliation of pillared-layer metal-organic framework to boost the oxygen evolution reaction, *Angew. Chem., Int. Ed.*, 2018, **57**, 4632–4636.

34 Y. Ding, Y. P. Chen, X. Zhang, L. Chen, Z. Dong, H. L. Jiang, H. Xu and H. C. Zhou, Controlled intercalation and chemical exfoliation of layered metal-organic frameworks using a chemically labile intercalating agent, *J. Am. Chem. Soc.*, 2017, **139**, 9136–9139.

35 E. Y. Choi, K. Park, C. M. Yang, H. Kim, J. H. Son, S. W. Lee, Y. H. Lee, D. Min and Y. U. Kwon, Benzene-templated hydrothermal synthesis of metal-organic frameworks with selective sorption properties, *Chemistry*, 2004, **10**, 5535–5540.

36 V. Guillerm, H. Xu, J. Albalad, I. Imaz and D. Maspoch, Postsynthetic selective ligand cleavage by solid-gas phase ozonolysis fuses micropores into mesopores in metal-organic frameworks, *J. Am. Chem. Soc.*, 2018, **140**, 15022–15030.

37 J. Albalad, H. Xu, F. Gándara, M. Haouas, C. Martineau-Corcos, R. Mas-Ballesté, S. A. Barnett, J. Juanhuix, I. Imaz and D. Maspoch, Single-crystal-to-single-crystal postsynthetic

modification of a metal-organic framework *via* ozonolysis, *J. Am. Chem. Soc.*, 2018, **140**, 2028–2031.

38 B. Cochran, One-pot oxidative cleavage of olefins to synthesize carboxylic acids by a telescoped ozonolysis-oxidation process, *Synlett*, 2015, **27**, 245–248.

39 B. L. Chen, S. Q. Ma, F. Zapata, E. B. Lobkovsky and J. Yang, Hydrogen adsorption in an interpenetrated dynamic metal-organic framework, *Inorg. Chem.*, 2006, **45**, 5718–5720.

40 B. L. Chen, F. R. Fronczek, B. H. Courtney and F. Zapata, α-Po nets of copper(II)-trans-1,4-cyclohexanedicarboxylate frameworks based on a paddle-wheel building block and its enlarged dimer, *Cryst. Growth Des.*, 2006, **6**, 825–828.